

UCLA

UCLA Previously Published Works

Title

Transcatheter Aortic Valve Replacement Guided by Preprocedural Simulation of Fluoroscopic Location of the Membranous Septum.

Permalink

<https://escholarship.org/uc/item/753771sj>

Authors

Mori, Shumpei
Aksoy, Olcay
Do, Duc H
et al.

Publication Date

2023-06-01

DOI

10.1016/j.jaccas.2023.101888

Copyright Information

This work is made available under the terms of a Creative Commons Attribution-NonCommercial-NoDerivatives License, available at <https://creativecommons.org/licenses/by-nc-nd/4.0/>

Peer reviewed

CASE REPORT

ADVANCED

CLINICAL CASE

Transcatheter Aortic Valve Replacement Guided by Preprocedural Simulation of Fluoroscopic Location of the Membranous Septum



Shumpei Mori, MD, PhD,^a Olcay Aksoy, MD,^b Duc H. Do, MD, MS,^a Ravi H. Dave, MD,^b Kalyanam Shivkumar, MD, PhD^{a,b}

ABSTRACT

We show the virtual simulation of the fluoroscopic location of the membranous septum using preprocedural cardiac computed tomographic data sets. Recognizing the risk distance before the procedure can help individualize implantation strategy to reduce the risk of atrioventricular conduction axis damage during transcatheter aortic valve replacement. **(Level of Difficulty: Advanced.)** (J Am Coll Cardiol Case Rep 2023;16:101888) © 2023 The Authors. Published by Elsevier on behalf of the American College of Cardiology Foundation. This is an open access article under the CC BY-NC-ND license (<http://creativecommons.org/licenses/by-nc-nd/4.0/>).

A 72-year-old woman with body mass index of 37.9 kg/m² was admitted with worsening shortness of breath and nonradiating chest and epigastric pain with exertion. On admission, her blood pressure was 138/64 mm Hg, her pulse was 72 beats/min and regular, she was afebrile, and her oxygen saturation was 96% on room air. Her clinical

examination revealed a Levine III/VI systolic ejection murmur, which was most prominent at the right sternal boarder of the second intercostal space. Her lung sounds were clear. Bilateral lower extremity pitting edema was present.

MEDICAL HISTORY

The patient had a history of hypertension, hyperlipidemia, type 2 diabetes mellitus, gastroesophageal reflux disease, psoriasis, anemia, and liver cirrhosis secondary to nonalcoholic steatohepatitis.

DIFFERENTIAL DIAGNOSIS

The differential diagnoses included aortic stenosis, chronic heart failure, decompensated heart failure,

LEARNING OBJECTIVES

- To be able to appreciate the importance of recognizing individual risk distance before the procedure.
- To understand the utility and feasibility of preprocedural 'virtual simulation' of the membranous septum.

From the ^aUCLA Cardiac Arrhythmia Center, UCLA Health System, David Geffen School of Medicine at UCLA, Los Angeles, California, USA; and the ^bUCLA Cardiovascular Interventional Programs, David Geffen School of Medicine at UCLA and UCLA Health System, Los Angeles, California, USA.

Sei Iwai, MD, served as Guest Associate Editor for this paper. John W. Hirshfeld, Jr, MD, served as Guest Editor-in-Chief for this paper.

The authors attest they are in compliance with human studies committees and animal welfare regulations of the authors' institutions and Food and Drug Administration guidelines, including patient consent where appropriate. For more information, visit the [Author Center](#).

Manuscript received October 19, 2022; revised manuscript received February 15, 2023, accepted March 1, 2023.

**ABBREVIATIONS
AND ACRONYMS****AV** = atrioventricular**TAVR** = transcatheter aortic valve replacement

angina pectoris, pulmonary thromboembolism, gastroesophageal reflux disease, peptic ulcer, and gastrointestinal bleeding.

INVESTIGATIONS

An electrocardiogram demonstrated normal sinus rhythm with narrow QRS complex (QRS width, 98 ms), leftward axis (QRS axis, -25°), and without atrioventricular (AV) conduction block (P-R interval, 175 ms). Transthoracic echocardiography revealed normal left ventricular ejection fraction (65%) with left ventricular hypertrophy (ventricular septal thickness, 12 mm; inferolateral wall thickness, 14 mm). Doppler findings (peak flow velocity, 4.3 m/s; mean pressure gradient, 52.0 mm Hg) were consistent with severe aortic stenosis. By use of the continuity equation formula, the aortic valve area was calculated as 0.92 cm^2 (index $0.41 \text{ cm}^2/\text{m}^2$). There was mild to moderate aortic regurgitation.

Preprocedural analyses of the aortic root and vascular access routes were performed with cardiac computed tomography. Additionally, to evaluate the fluoroscopic location of the AV conduction axis, which is usually located at the inferior margin of the membranous septum,¹⁻⁵ we reconstructed virtual fluoroscopic images with the aortic root, membranous septum, and virtual basal ring (Figure 1, Video 1). The systolic data set (39% of the R-R interval) was used for

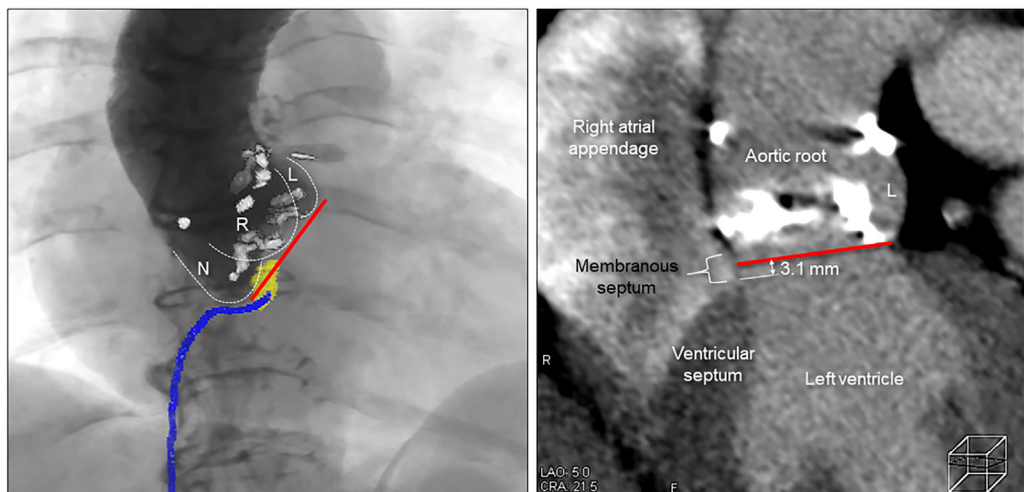
reconstruction. This virtual fluoroscopic simulation visually confirmed the short vertical distance between the virtual basal ring and the inferior margin of the membranous septum (risk distance), measured at 3.1 mm (Figure 1). Furthermore, a virtual His-bundle electrode was reconstructed at the inferior margin of the membranous septum (Figures 1 and 2, Video 1). All analyses were performed with a commercially available workstation (Ziostation2 version 2.9.7.1).

MANAGEMENT

Transfemoral transcatheter aortic valve replacement (TAVR) was performed while the patient was under sedation with single-plane fluoroscopy. Invasive coronary angiography before the procedure revealed no significant stenosis in either the right or the left coronary arteries.

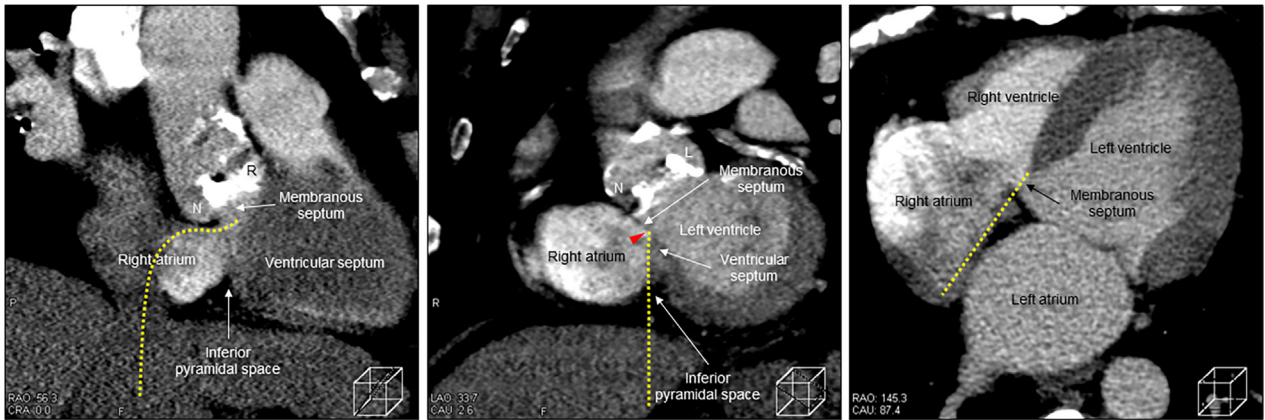
Initially, a His-bundle (5-F 5-5-5 CRD-2, Abbott) and right ventricular apical (5-F 5-5-5 CRD, Abbott) quadripolar catheters were placed to mark the location of the AV conduction axis and to perform an electrophysiology study. The location of the His-bundle electrode was compatible with that indicated by the virtual simulation (Figure 1).

At baseline, the patient exhibited slight prolongation in the A-H interval (146 ms), normal H-V interval (45 ms), and normal QRS width (98 ms), with a sinus cycle length of 1,200 ms (Figure 3).

FIGURE 1 Simulation of Fluoroscopic Location of the Membranous Septum

Left panel shows virtual simulation of the membranous septum (yellow) in relation to aortography with calcification (white), virtual basal ring (red), and cardiac contour viewed from the right anterior oblique 17° and caudal 5° perpendicular view. Virtual His-bundle catheter (blue) is also reconstructed. The orthogonal distance between the virtual basal ring (red) and the inferior margin of the membranous septum (risk distance) is as short as 3.1 mm (right). Refer to Video 1. L = left coronary aortic sinus; N = noncoronary aortic sinus; R = right coronary aortic sinus.

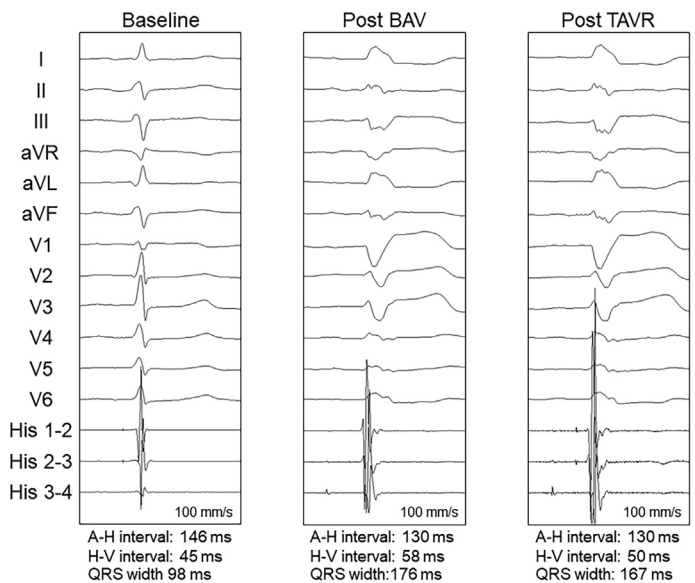
FIGURE 2 Multiplanar Reconstruction Images Used to Reconstruct Virtual His-Bundle Electrode



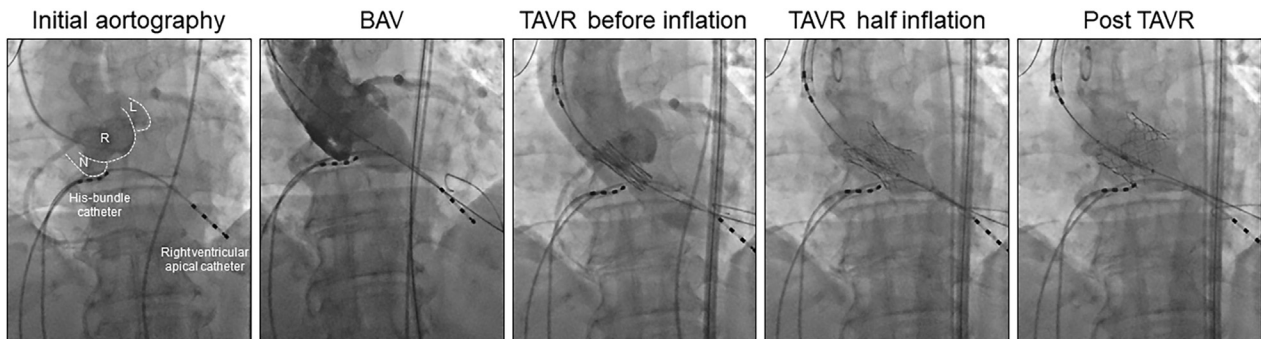
The multiplanar reconstruction images correspond to right anterior oblique view (**left**), left anterior oblique view (**middle**), and horizontal view (**right**) to simulate the virtual His-bundle electrode location (**yellow dotted line**). Three-dimensional information of this yellow dotted line is reconstructed to the virtual His-bundle electrode in **Figure 1** and **Video 1**. **Red arrowhead** denotes the angulation created between the membranous septum and the crest of the ventricular septum, where the His-bundle electrode is generally fixed. L = left coronary aortic sinus; N = noncoronary aortic sinus; R = right coronary aortic sinus.

There was no retrograde conduction at baseline and no antegrade dual AV nodal physiology. The antegrade Wenckebach cycle length was 400 ms. Aortography showing a perpendicular view confirmed the short risk distance (**Figure 4**) as suggested by preprocedural virtual simulation. Immediately after the balloon aortic valvuloplasty with a 25-mm balloon under rapid right ventricular apical pacing (180 beats/min) (**Figure 4**), complete left bundle branch block developed (QRS width, 176 ms) with slight prolongation in the H-V interval (58 ms) (**Figure 3**). A 26-mm Edwards SAPIEN 3 (Edwards Lifesciences) valve was then deployed under rapid right ventricular apical pacing (180 beats/min). The valve was positioned to achieve an implantation depth of 0 to approximately 2 mm using the His-bundle electrode as a landmark (**Figure 4**). The TAVR procedure was then terminated without postdilatation owing to persistence of complete left bundle branch block after the balloon valvuloplasty and optimal implantation results (postprocedural peak flow velocity, 2.6 m/s; mean pressure gradient, 13.0 mm Hg; trace paravalvular aortic regurgitation). Electrophysiological study immediately after valve deployment showed persistent slight prolongation in the A-H interval (130 ms), normal H-V interval (50 ms), and complete left bundle branch block (QRS width, 167 ms), with a sinus cycle length of

FIGURE 3 Temporal Change of the Electrocardiogram and His-Bundle Electrogram During the Procedure



After the balloon aortic valvuloplasty (BAV), complete left bundle branch block developed with slight prolongation in the H-V interval. Electrocardiographic findings immediately after valve deployment confirmed that further mechanical damage to the atrioventricular conduction axis was successfully avoided. TAVR = transcatheter aortic valve replacement.

FIGURE 4 Fluoroscopic Images During the Procedure Viewed From Perpendicular View

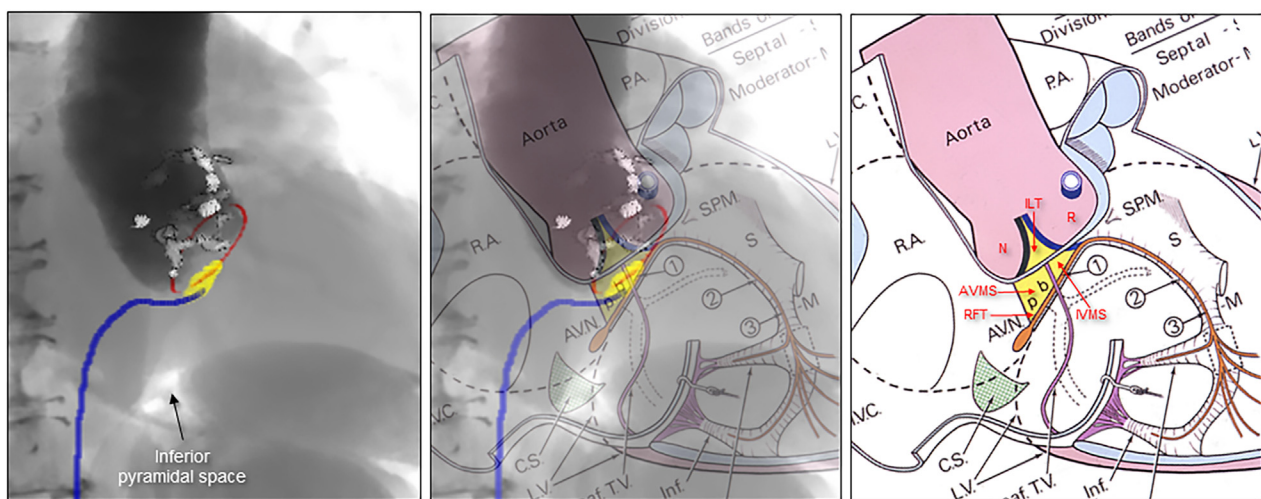
Perpendicular view (right anterior oblique 20° and caudal 13°) was set with the right coronary aortic sinus located centrally. The valve was positioned just above the His-bundle electrode to achieve an implantation depth of 0~2 mm. Note the relationship between the His-bundle electrode and aortic root and catheter-based artificial aortic valve. Compare with [Figure 1A](#). BAV = balloon aortic valvuloplasty; L = left coronary aortic sinus; N = noncoronary aortic sinus; R = right coronary aortic sinus; TAVR = transcatheter aortic valve replacement.

1,080 ms ([Figure 3](#)). The antegrade Wenckebach cycle length was 460 ms. On the basis of on these findings, a temporary pacemaker was not placed. The patient's postprocedural clinical course was uneventful, with prompt return of normal AV conduction by the next morning. An electrocardiogram before discharge demonstrated normal sinus rhythm with narrow QRS complex (QRS width, 100 ms),

leftward axis (QRS axis, -14°), and without AV conduction block (P-R interval, 188 ms).

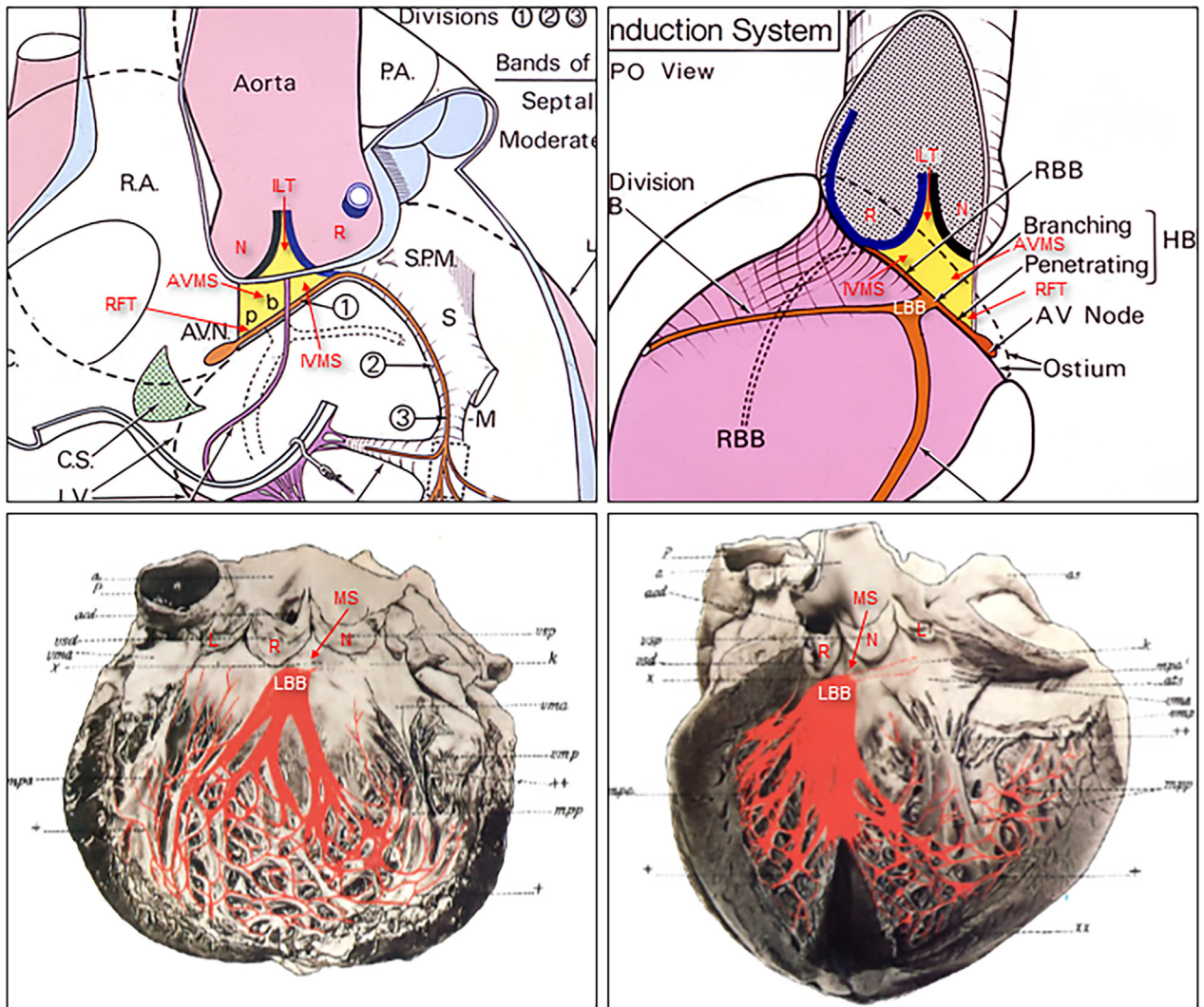
DISCUSSION

TAVR has revolutionized the care of patients with aortic stenosis. However, the risk of mechanical damage to the AV conduction axis remains a

FIGURE 5 Structural Anatomy Around the Membranous Septum

Fusion image ([middle](#)) between computed tomographic image ([left](#)) and illustration by Wallace A. McAlpine ([right](#)).⁴ [Left](#), virtual fluoroscopic simulation image with the membranous septum ([yellow](#)), calcification ([white](#)), virtual basal ring ([red](#)), and virtual His-bundle electrode ([blue](#)) viewed from the right anterior oblique 45°. Illustration courtesy of UCLA Cardiac Arrhythmia Center, Wallace A. McAlpine MD Collection. Note that explaining every original abbreviation is outside the scope of this paper. [Red](#) annotations are additionally inserted. AVMS = atrioventricular portion of the membranous septum; ILT = interleaflet triangle; IVMS = interventricular portion of the membranous septum; MS = membranous septum; N = noncoronary aortic sinus; R = right coronary aortic sinus; RFT = right fibrous trigone.

FIGURE 6 Structural Anatomy of the Conduction System



Anatomy of the conduction system illustrated by Wallace A. McAlpine (above).⁴ This is a stylized example of the branching patterns of the left bundle branch. Note the significant difference in the location of the branching bundle and base of the left bundle branch relative to the right and noncoronary aortic sinuses with the illustration by Sunao Tawara (below).² Explaining every original abbreviation is outside the scope of this paper. Red and white annotations are additionally inserted. AVMS = atrioventricular portion of the membranous septum; ILT = interleaflet triangle; IVMS = interventricular portion of the membranous septum; L = left coronary aortic sinus; LBB = left bundle branch; MS = membranous septum; N = noncoronary aortic sinus; R = right coronary aortic sinus; RFT = right fibrous trigone. Illustrations in top row courtesy of UCLA Cardiac Arrhythmia Center, Wallace A. McAlpine MD Collection.

significant challenge.¹ Prevention of such damage requires precise knowledge of the relevant structural anatomy in each case.²⁻⁵

We demonstrate the utility and feasibility of virtual simulation of fluoroscopic location of the membranous septum to prevent AV conduction damage. The anatomical accuracy of virtual simulation was confirmed by a real His-bundle electrode. We believe that virtual simulation of fluoroscopic location of the membranous septum should enhance the safety of the

procedure, mitigating the risk of AV conduction damage and need for permanent pacemaker implantation.

As TAVR techniques mature and its indications are broadened,¹ clinical anatomy around the aortic root has been increasingly studied.⁶⁻⁹ It is now generally accepted that individual adjustment of the implantation depth relative to each risk distance can lead to reduction of permanent pacemaker implantation.¹⁻⁶ Thus, 3-dimensional preprocedural understanding of the fluoroscopic location of the membranous septum

is of paramount importance (Figures 5 and 6). With the availability of software systems, the reconstruction of the virtual basal ring and its relationship to the membranous system is readily feasible for each patient, further allowing us to individualize this highly variable relationship.⁶⁻⁹ Such detailed analyses have shown that, in some cases, the virtual basal ring is located within the membranous septum; thus, the “height” of the membranous septum does not always represent the risk distance.⁶⁻⁸ This risk distance (Figure 1) is commonly ≤ 5 mm. This distance is a practical matter, given that a shorter distance may be associated with a higher risk of pacemaker implantation,⁷ especially in cases of larger implantation depth.⁸ In addition, if the risk distance is negative,⁷ (ie, the membranous septum is located superior to the virtual basal ring), the potential risk of AV conduction axis damage is likely to increase significantly. Considering this variation, further improvements of the device itself or fine adjustments of the implantation technique are required to customize the TAVR procedure. Additionally, individualized risk can be provided to each patient by measuring this distance before TAVR.

It is notable that the virtual basal ring reconstructed by computed tomography is lower than that defined by aortography, because the latter does not account for the thickness of the wall of the aortic root, which is generally <1.0 mm. This provides a subtle but additional safety margin to the risk distance measured by computed tomography.

Moreover, the inferior margin of the anterosuperior part of the membranous septum becomes much closer to the virtual basal ring (Figure 5, Video 1) than that of the posteroinferior part. In fact, this part of the membranous septum is located at the level of, or superior to, the virtual basal ring in 66% to 78% of adult hearts.^{6,8} In such cases, the AV conduction axis is likely to be impinged upon by the strut,⁶ even if the prosthesis was placed with zero implantation depth. However, the location of the branching portion of the AV bundle does not always extend to cover the entire inferior margin of the membranous septum. The extent of branching portion relative to the membranous septum and morphology of the proximal left bundle branch show wide variations.^{2,5,10} Although the importance of the risk distance at the anterosuperior part of the membranous septum on AV conduction damage during TAVR was recently reported,¹¹ anatomical nuances around the membranous septum¹² and their clinical impact on TAVR require further investigation. Therefore, preprocedural virtual simulation of the membranous septum may provide some additional confidence to

intentionally avoid inadvertent damage to the AV conduction axis.

The utility and feasibility of simultaneous electrophysiological study during TAVR have been evaluated.¹² After implantation of catheter-based artificial aortic valves, significant prolongation in the H-V interval (47 ± 8 ms to 56 ± 12 ms), antegrade Wenckebach point (334 ± 45 ms to 354 ± 41 ms), and QRS duration (109 ± 27 ms to 117 ± 30 ms) were observed.¹³ These changes were mostly infranodal but temporary, which are similar to the present case. Although the efficacy and feasibility of His-bundle electrode-guided TAVR needs further investigation, virtual simulation of the membranous septum can partially replace its role by suggesting and visualizing the risk distance in preprocedural 3-dimensional fashion. Larger prospective studies will be necessary to assess the utility and feasibility of this technique.

FOLLOW-UP

The patient's post-discharge course was uneventful during 23 months of follow-up, with an improvement in her shortness of breath. Transthoracic echocardiography 20 months after TAVR maintained optimal results: peak flow velocity, 2.7 m/s; mean pressure gradient, 14.0 mm Hg; and no paravalvular aortic regurgitation. The electrocardiogram 23 months after TAVR also confirmed optimal results: normal sinus rhythm; QRS width, 98 ms; QRS axis, -19° ; and P-R interval, 180 ms.

CONCLUSIONS

This case highlights the use of computed tomographic 3-dimensional virtual simulation of the AV conduction axis location, using the membranous septum as the indicator. The images should be shared among the members of the heart team to provide an individualized strategy to reduce the risk of AV block.

FUNDING SUPPORT AND AUTHOR DISCLOSURES


This work was made possible by support from NIH grants OT2OD023848 to Dr Shivkumar. All other authors have reported that they have no relationships relevant to the contents of this paper to disclose.

ADDRESS FOR CORRESPONDENCE: Dr. Shumpei Mori, UCLA Cardiac Arrhythmia Center, UCLA Health System, David Geffen School of Medicine at UCLA, Center of Health Sciences, Suite 46-119C, 650 Charles E. Young Drive South, Los Angeles, California 90095, USA. E-mail: smori@mednet.ucla.edu. Twitter: [@shivkumarmd](https://twitter.com/shivkumarmd).

REFERENCES

1. van der Boon RM, Nuis RJ, Van Mieghem NM, et al. New conduction abnormalities after TAVI: frequency and causes. *Nat Rev Cardiol*. 2012;9:454–463.
2. Tawara S. *Das Reizleitungssystem Des Säugetierherzens. Eine Anatomisch-Histologische Studie Über das Atrioventrikulärbündel und die Purkinjischen Fäden*. Gustav Fischer; 1906.
3. Widran J, Lev M. The dissection of the atrioventricular node, bundle and bundle branches in the human heart. *Circulation*. 1951;4:863–867.
4. McAlpine WA. *Heart and Coronary Arteries: An Anatomical Atlas for Clinical Diagnosis, Radiological Investigation, and Surgical Treatment*. Springer; 1975.
5. Massing GK, James TN. Anatomical configuration of the His bundle and bundle branches in the human heart. *Circulation*. 1976;53:609–621.
6. Kawashima T, Sato F. Visualizing anatomical evidences on atrioventricular conduction system for TAVI. *Int J Cardiol*. 2014;174:1–6.
7. Mori S, Tretter JT, Toba T, et al. Relationship between the membranous septum and the virtual basal ring of the aortic root in candidates for transcatheter implantation of the aortic valve. *Clin Anat*. 2018;31:525–534.
8. Tretter JT, Mori S, Anderson RH, et al. Anatomical predictors of conduction damage after transcatheter implantation of the aortic valve. *Open Heart*. 2019;6:e000972.
9. Jilaihawi H, Zhao Z, Du R, et al. Minimizing permanent pacemaker following repositionable self-expanding transcatheter aortic valve replacement. *J Am Coll Cardiol Interv*. 2019;12:1796–1807.
10. Elizari MV. The normal variants in the left bundle branch system. *J Electrocardiol*. 2017;50:389–399.
11. Jørgensen TH, Hansson N, De Backer O, et al. Membranous septum morphology and risk of conduction abnormalities after transcatheter aortic valve implantation. *EuroIntervention*. 2022;17:1061–1069.
12. Mori S, Hanna P, Bhatt RV, Shivkumar K. The atrioventricular bundle: a sesquicentennial tribute to Professor Sunao Tawara. *J Am Coll Cardiol EP*. 2023;9:444–447.
13. Eksik A, Gul M, Uyarel H, et al. Electrophysiological evaluation of atrioventricular conduction disturbances i transcatheter aortic valve implantation with Edwards SAPIEN prosthesis. *J Invasive Cardiol*. 2013;25:305–309.

KEY WORDS atrioventricular conduction axis, computed tomography, membranous septum, transcatheter aortic valve replacement, virtual basal ring

 **APPENDIX** For supplemental video, please see the online version of this paper.